



Cite this: *CrystEngComm*, 2015, 17, 8011

Received 4th April 2015,  
Accepted 30th April 2015

DOI: 10.1039/c5ce00662g

www.rsc.org/crystengcomm

# Influence of chiral ligands on the gel formation of a Mg(II) coordination polymer†

Wei Lee Leong,<sup>a</sup> Sudip K. Batabyal,<sup>a</sup> Stefan Kasapis<sup>b</sup> and Jagadese J. Vittal<sup>\*a</sup>

The self-assembly of Mg<sup>2+</sup> ions and *N*-(7-hydroxyl-4-methyl-8-coumarinyl)-alanine furnished mesoscale assembled structures as microfibres comprising well-aligned nanofibres or a randomly cross-linked gel network depending on the pH of the solution and the chirality of the ligand used. Formation of a diastereomer during complexation is responsible for this behavior.

A gel is a soft solid containing mostly-immobilized liquid inside a cross-linked network formed by gelator molecules. These gelators are mostly low molecular weight organic molecules. Such gels have a wide range of practical applications in cosmetics, contact lenses, drug delivery and bio-medical applications.<sup>1–7</sup> Recently, metal complexes and coordination polymers have also been used as gelators and the resultant gels are known as metallo gels<sup>8</sup> and coordination polymeric gels.<sup>9</sup> The chirality of the molecules has a major effect on the aggregated morphology. In general, small chiral molecules self-assemble into chiral aggregates which further give rise to helical aggregates.<sup>10</sup> Hence it is not surprising that chiral organic gelators and chiral ligands have been employed to investigate their influence on the self-assembly of supramolecular chiral gels.<sup>11–18</sup> Several of these studies have yielded not only helical structures but also very interesting physical properties.<sup>8,9</sup> However, the influence of enantiomers and diastereomers on the properties of the supramolecular gel has rarely been explored. The amide formed between lauryl chloride and (1*R*,2*R*)-1,2-diaminocyclohexane has been reported to form gels in a variety of solvents. The corresponding (1*S*,2*S*)-derivative was also found to form gels under similar conditions and the CD spectra of both enantiomeric compounds are mirror images of each other.<sup>19</sup>

Herein, we describe a simple way to orientate coordination polymeric chains by controlling the chirality of the ligand and pH of the solution. Previously, we have reported that the self-assembly of Mg<sup>2+</sup> ions and *N*-(7-hydroxyl-4-methyl-8-coumarinyl)-L-alanine (H<sub>2</sub>L-muala) furnished a pH- and mechano-responsive coordination polymeric hydrogel.<sup>20</sup> Here, we observed that the corresponding H<sub>2</sub>D-muala ligand produces a macroscale fibre coordination polymer by hierarchical assembly from nanofibres to a fibre-like morphology at millimeter scale. More interestingly, variation of the solution pH afforded another type of aggregation, forming a hydrogel, which is similar to the behavior of the H<sub>2</sub>L-muala ligand.

When an aqueous solution of H<sub>2</sub>D-muala and two equivalents of LiOH was reacted with Mg(CH<sub>3</sub>COO)<sub>2</sub>·4H<sub>2</sub>O, a clear yellow solution was obtained at pH 10. Instead of gelation, which occurred for the H<sub>2</sub>L-muala analogue,<sup>20</sup> the clear solution turned into yellowish fibrous fibre 1 suspended in solution. The fibres became thicker with time as more molecules assembled on them. On standing for about 24 h, the fibre could not freely stand and collapsed like cotton-pulp. Fig. 1 left shows the evolution of nanofibres into microfibres at different time intervals. The product Mg(D-muala) is expected to display a 1D coordination polymeric structure through

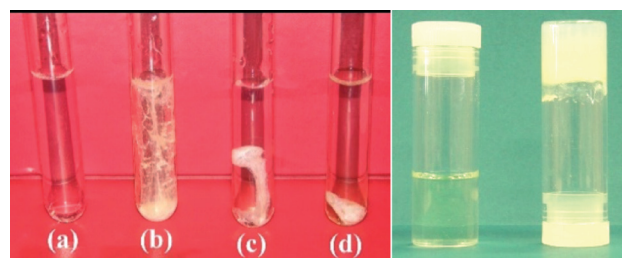


Fig. 1 Left: Evolution of nanofibres into microfibres at (a) 0 h, (b) 5 h, (c) 24 h and (d) 2 weeks. Right: A photograph showing the solution mixture of ligands and Mg<sup>2+</sup> ions in the presence of two (left) and three (right) equivalents of LiOH, showing the formation of a solution and a gel, respectively.

<sup>a</sup> 3 Science Drive 3, Department of Chemistry, National University of Singapore, Singapore 117543. E-mail: chmjv@nus.edu.sg; Fax: +65 6779 1691; Tel: +65 6516 2975

<sup>b</sup> School of Applied Sciences, RMIT University, City Campus, Melbourne, Victoria 3001, Australia. Tel: +61 3 9925 5244

† Electronic supplementary information (ESI) available: Experimental procedure, FTIR, ESI-MS, SEM, PXRD, UV-vis and PL spectra. See DOI: 10.1039/c5ce00662g



carboxylate bridging. It appears that these 1D polymer chains formed initially at the nanoscale are bundled up through hydrogen bonding interactions to form microfibrils. The differences in the behaviour of the enantiomeric muala ligands towards  $\text{Mg}^{2+}$  ions, one forming a gel while another results in microfibrils, is striking. It may be noted that *N*-(7-hydroxyl-4-methyl-8-coumarinyl)-glycine produced a hydrogel while  $\text{H}_2\text{L}$ -muala resulted in a crystalline coordination polymer with  $\text{Zn}^{2+}$  ions.<sup>21</sup>

We further explored the possibility of obtaining the hydrogel with  $\text{H}_2\text{D}$ -muala by varying the experimental conditions such as the concentration and the pH of the solution. A stable hydrogel 28 wt% was successfully obtained using three equivalents of LiOH to deprotonate the  $\text{H}_2\text{D}$ -muala ligand before reaction with  $\text{Mg}(\text{CH}_3\text{COO})_2 \cdot 4\text{H}_2\text{O}$ . Fig. 1 right shows the photograph of the solution containing  $\text{H}_2\text{D}$ -muala and  $\text{Mg}^{2+}$  salt in the presence of three equivalents of LiOH upon mixing. Interestingly, a slight variation of the pH of the solution from 10 to 11 with LiOH led to instant formation of hydrogelation of 2, demonstrating the ability of the  $[\text{Mg}(\text{D-muala})]$  coordination polymer to form entirely different types of aggregation. Two equivalents of LiOH initially furnished a clear yellow solution and slowly turned to microfibrils upon aging (Fig. 1 left). The gelation has been confirmed by the inverted test tube method (Fig. 1 right). Similar to related hydrogels reported earlier,<sup>20</sup> the hydrogel 2 is also pH- and mechano-responsive. The hydrogel converts to a clear yellow solution in acidic pH, but recovers its gel structure at basic pH. In addition, it flows under vigorous shaking and recovers its gel structure upon standing. It is worth noting that the  $[\text{Mg}(\text{L-muala})]$  reaction mixture forms a hydrogel in the presence of two and three equivalents of LiOH,<sup>20</sup> which is quite different from the aggregation behavior of  $[\text{Mg}(\text{D-muala})]$ .

Control experiments have been conducted to investigate the effect of chirality of the muala ligand and pH on the self-assembly of  $[\text{Mg}(\text{muala})]$ . A racemic ligand  $\text{H}_2\text{DL}$ -muala was reacted with  $\text{Mg}^{2+}$  ions in the presence of two and three equivalents of LiOH. It was found that the solution mixture remained homogenous, even after aging for a few weeks. Hence it is concluded that a purely enantiomeric ligand is necessary to direct the self-assembly of 1D coordination polymers into a 3D entangled network.

The aggregation of  $[\text{Mg}(\text{D-muala})]$  was only observed in aqueous solution while a methanolic solution yielded a precipitate 3 after slow evaporation. Elemental analyses of all the products gives a composition of  $[\text{Mg}(\text{D-muala})(\text{H}_2\text{O})_2] \cdot 2\text{H}_2\text{O}$ . Furthermore, the FTIR spectra of dried 1 and 2 show identical absorption bands, suggesting the same composition of fibre 1 as hydrogel 2 (Fig. S2†). This reflects that the excess presence of LiOH only influences the aggregation state, and not the chemical composition. The IR spectra of both products display a broad absorption band around  $3435\text{ cm}^{-1}$  corresponding to the presence of water molecules. These water molecules are due to the coordinated water as the  $\text{Mg}^{2+}$  centers require two more ligands to complete the preferred

octahedral geometry, as well as lattice water. The difference in asymmetric and symmetric stretching frequencies of the carboxylate group in both fibre and gel were found to be around  $120\text{ cm}^{-1}$ , suggesting the bridging coordination mode for the carboxylate groups.<sup>24</sup> The carboxylate bridging is responsible for the 1D coordination polymer formation. These coordination polymers aggregate and bundle to form nanofibres and fibrous nanostructures. 1 and 2 also exhibit similar ESI-MS spectra, further proving that these two compounds have the same chemical composition. The major peaks in the mass spectra can be assigned to  $[\text{D-muala}]$ ,  $[\text{Mg}(\text{D-muala})(\text{solvent})_x]$  and  $[\text{Mg}_2(\text{D-muala})_2(\text{solvent})_x]$  (Fig. S3†).

Field emission scanning electron microscopy was used to gain insight into the microscopic morphology of the fibre 1 and the gel 2. Fig. 2a and b show typical SEM images of a fibre sample which consists of large quantities of well-defined nanowires with lengths of several microns and a diameter of  $\sim 100\text{ nm}$ . These individual nanofibres were laterally aggregated into microscale fibres. These microfibrils are quite big and have low porosity. Less water could be trapped within the porous network, and so no stable hydrogel could be formed.

On the other hand, hydrogel 2 displays a nanofibrous network structure as shown in Fig. 2c and d. The fibres are randomly oriented, which is quite obvious for gel formation. The nanofibres are in the range of 5–10 microns in length and 50–100 nm in diameter. The presence of multiple hydrogen bonding functionalities facilitated the entanglement of nanofibres to assemble into a 3D network. Such a porous network can entrap water molecules to form a hydrogel. It may be noted that the fibrous network is confined to a sheet-like morphology. This is different from the previous hydrogel  $[\text{Mg}(\text{L-muala})(\text{H}_2\text{O})_2] \cdot n\text{H}_2\text{O}$ , which exhibits a nanoribbon fibrous 3D porous network.<sup>20</sup> SEM images of 1 under

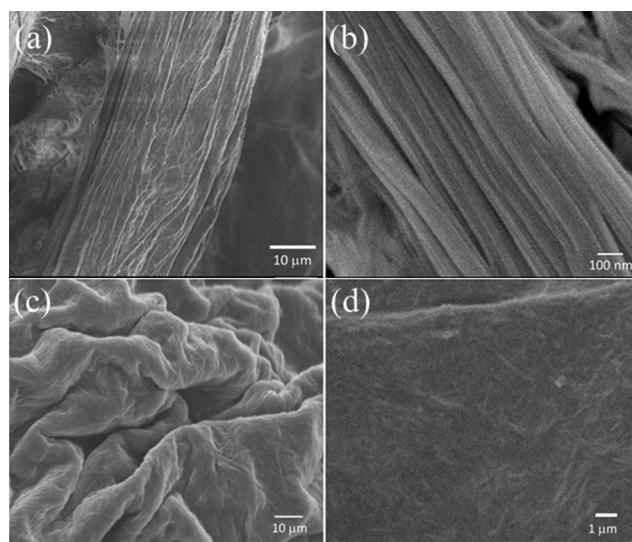


Fig. 2 SEM micrographs of fibre 1 at two different magnifications (a) and (b); SEM micrographs of freeze dried 2 at two different magnifications (c) and (d).



different magnifications are shown in Fig. S4†. Such nanofibre assemblies have been actively pursued for various applications.<sup>22,23</sup> Compound 3 is a powder, with no well-defined alignment or fibrous network (Fig. S5†).

It is interesting to find that the microfibrils (fibre) formed from the nanoscale assemblies of nanofibres transformed into nanofibrous random networks (gel) simply by changing the pH of the solution. Moreover, the change of chirality of the amino acid backbone in muala from L to D dramatically influences the transformation of hydrogel to microfibrils under the same experimental conditions. A quick search of the literature revealed that an optically active  $\pi$ -conjugated poly(azomethine) derivative exhibits supramolecular self-assembled fibrous structures whereas the corresponding racemic analogue poly(azomethine) assembled into nanoparticle form.<sup>25</sup>

X-ray powder diffraction patterns of 1 and 2 disclose the essentially amorphous nature of the self-assembled products (Fig. S6†). The peaks at  $\sim 14^\circ$  correspond to a spacing of 6.5 Å, which could be a metal-metal vector in the proposed polymer (Fig. S8†). Slow aggregation of the nanofibres from the mother liquor appears to be responsible for the short-range ordered alignment of microfibre 1 and hence its crystallinity, while it is surprising that the instant gelation of 2, which resulted from the random cross-linking of nanofibres, also has a similar crystalline nature. It is probable that 2 might have acquired some crystallinity during the freeze-dry process to get the dried powder.

Fluorescence properties of 1 and 2 have been investigated. The fluorescence spectrum of the aqueous solution of 1 shows strong emission around 445 nm. The hydrogel 2 also exhibits remarkable blue emission at 450 nm in the same region (Fig. 3a). The strong fluorescence properties of 1 and 2 correspond to the  $\pi$ - $\pi^*$  transition in the coumarin functionalities. The hydrogel 2 shows blue emission under UV light (Fig. 3b). Both 1 and 2 display remarkable fluorescence enhancement compared to the free ligand (Fig. S13†). It may be attributed to the rigidification of the medium upon gelation which slows down nonradiative decay that leads to

fluorescence enhancement.<sup>26</sup> Such fluorescence enhancement has been observed before.<sup>20,21</sup>

Rheological studies have been performed to elucidate the mechanical properties of the gel. This can be carried out using dynamic oscillation which gives information about viscous and elastic properties of the materials. The storage (or elastic) modulus  $G'$  represents the solid-like character and energy stored while the loss (or viscous) modulus  $G''$  reflects the liquid-like behavior and energy lost.

The frequency sweep of hydrogel 2 is shown in Fig. 4a. The in-phase storage modulus  $G'$  which indicates its elastic properties is about one order of magnitude higher than the out-of-phase loss modulus  $G''$  over the whole frequency range, an indication of a weak gel-like structure. It should be noted that the  $G'$  value of 420 Pa is significantly less than that of the related Mg hydrogel obtained from L-muala.<sup>20</sup> This suggests that the gel formed by [Mg(D-muala)] is much weaker than that formed by [Mg(L-muala)]. Nonetheless, the  $G'$  is similar to the Zn hydrogel obtained from mugly.<sup>21</sup> These observations suggest that the chirality in amino acid influences the aggregation greatly, which ultimately determines the gel or fibre formation and the strength of the entangled network. The dynamic strain sweep of hydrogel 2 was determined with a strain amplitude ranging from 0.1% to 2000% at 1 rad s<sup>-1</sup> (Fig. 4b). Both  $G'$  and  $G''$  remain constant up to  $\sim 1\%$  strain ( $G' > G''$ ). Beyond this level, a disruption of the network occurs as shown by a dramatic drop in the values of both moduli and the reversal of the viscoelastic signal ( $G'' > G'$ ).

Finally a question remains to be answered as to why D-muala behaves differently from L-muala under the same experimental conditions, not forming a coordination polymeric gel. As shown in Fig. 5, the free H<sub>2</sub>D-muala ligand is an enantiomer with a chiral carbon atom and a prochiral nitrogen center. Once it forms a complex with Mg<sup>2+</sup> ion the nitrogen atom also becomes a chiral center, hence the ligand becomes a diastereomer. In another study, similar enantiomers L-sala and D-sala ligands upon complexation with Zn<sup>2+</sup> have C<sub>R</sub>N<sub>S</sub> and C<sub>S</sub>N<sub>R</sub> stereochemistry, respectively.<sup>27</sup> Hence, similar stereochemistry is also expected for the [Mg(D-muala)] and [Mg(L-muala)] complexes. Diastereomers are not expected

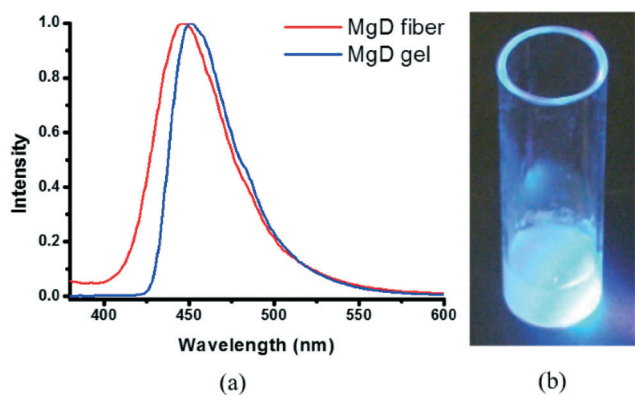


Fig. 3 (a) Fluorescence spectra of 1 and 2 upon excitation at  $\lambda = 360$  nm in aqueous solution; (b) photograph of hydrogel 2 under UV light.

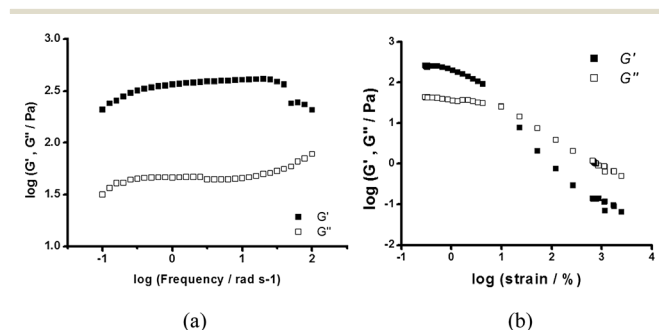


Fig. 4 (a) Dynamic frequency sweep measurements of  $G'$  and  $G''$  for hydrogel 2 at a strain of 0.1%. (b) Dynamic strain sweep of hydrogel 2 at 1 rad s<sup>-1</sup> and 25 °C.



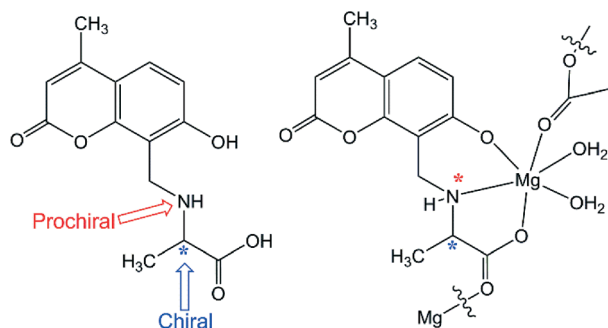


Fig. 5 Structural diagram of the D-muala ligand (left) and the proposed repeating unit of the coordination polymeric gel showing the chiral centers (right).

to show the same or similar physical properties. Hence it is not surprising that the D-muala ligand furnishes fibres while under the same experimental conditions L-muala forms a gel with  $\text{Mg}^{2+}$  ions.

In summary, *N*-(7-hydroxyl-4-methyl-8-coumarinyl)-D-alanine forms microfibrils and a hydrogel with  $\text{Mg}^{2+}$  in the presence of a base. The pH of the solution and chirality of amino acid influence the aggregation. L-muala produces a coordination polymeric gel while D-muala gives Mg nanofibres under the same experimental conditions through the formation of different diastereomers during complexation. An increase in pH leads to a coordination polymeric gel,  $[\text{Mg}(\text{D-muala})]$ , while no influence is seen for  $[\text{Mg}(\text{L-muala})]$ . These results show that the chirality of an amino acid could direct the topologies of a coordination polymer, which further influenced the aggregation at the nanoscale. Hydrogel formation is more favourable at high pH while D-muala can only produce a  $\text{Mg}^{2+}$  hydrogel in an excess of base. Both fibre and gel have the same chemical composition and fluorescence properties as evidenced by various spectroscopic characterizations. Interestingly D,L-muala does not yield a gel or nanofibres. This report demonstrates the alteration of nanoscale morphologies induced by chirality and pH as a potential method for smart control of the functions of nanomaterials.

## Acknowledgements

This work is supported by the Ministry of Education Singapore through a Tier 1 grant (grant no. R-143-000-604-112).

## References

- 1 E. Carretti, M. Bonini, L. Dei, B. H. Berrie, L. V. Angelova, P. Baglioni and R. G. Weiss, *Acc. Chem. Res.*, 2010, **43**, 751–760.
- 2 P. Dastidar, *Chem. Soc. Rev.*, 2008, **37**, 2699–2715.
- 3 M. George and R. G. Weiss, *Acc. Chem. Res.*, 2006, **39**, 489–497.
- 4 N. M. Sangeetha and U. Maitra, *Chem. Soc. Rev.*, 2005, **34**, 821–836.
- 5 O. Gronwald, E. Snip and S. Shinkai, *Curr. Opin. Colloid Interface Sci.*, 2002, **7**, 148–156.
- 6 D. J. Abdallah and R. G. Weiss, *Adv. Mater.*, 2000, **12**, 1237–1247.
- 7 P. Terech and R. G. Weiss, *Chem. Rev.*, 1997, **97**, 3133–3160.
- 8 A. Y.-Y. Tam and V. W.-W. Yam, *Chem. Soc. Rev.*, 2013, **42**, 1540–1567.
- 9 J. H. Jung, J. H. Lee, J. R. Silverman and G. John, *Chem. Soc. Rev.*, 2013, **42**, 924–936.
- 10 *Topics in Stereochemistry*, ed. M. Green, R. J. M. Nolte and E. W. Meijer, Wiley, New Jersey, 2003.
- 11 M. Dubey, A. Kumar, R. K. Gupta and D. S. Pandey, *Chem. Commun.*, 2014, **50**, 8144–8147.
- 12 U. K. Das and P. Dastidar, *Chem. – Eur. J.*, 2012, **18**, 13079–13090.
- 13 P. Sahoo, D. K. Kumar, S. R. Raghavan and P. Dastidar, *Chem. – Asian J.*, 2011, **6**, 1038–1047.
- 14 Q. Jin, L. Zhang, H. Cao, T. Wang, X. Zhu, J. Jiang and M. Liu, *Langmuir*, 2011, **27**, 13847–13853.
- 15 Y. He, Z. Bian, C. Kang and L. Gao, *Chem. Commun.*, 2010, **46**, 5695–5697.
- 16 Y. He, Z. Bian, C. Kang, Y. Cheng and L. Gao, *Chem. Commun.*, 2010, **46**, 3532–3534.
- 17 S. I. Kawano, N. Fujita and S. Shinkai, *J. Am. Chem. Soc.*, 2004, **126**, 8592–8593.
- 18 R. Oda, I. Huc and S. Candau, *Angew. Chem., Int. Ed.*, 1998, **37**, 2689–2691.
- 19 K. Hanabusa, M. Yamada, M. Kimura and H. Shirai, *Angew. Chem., Int. Ed. Engl.*, 1996, **35**, 1949–1951.
- 20 W. L. Leong, S. K. Batabyal, S. Kasapis and J. J. Vittal, *Chem. – Eur. J.*, 2008, **14**, 8822.
- 21 W. L. Leong, A. Y.-Y. Tam, S. K. Batabyal, L. W. Koh, S. Kasapis, V. W.-W. Yam and J. J. Vittal, *Chem. Commun.*, 2008, 3628–3630.
- 22 D. K. Smith, *Chem. Soc. Rev.*, 2009, **38**, 684–694.
- 23 C. C. Lee, C. Grenier, E. W. Meijer and A. P. H. J. Schenning, *Chem. Soc. Rev.*, 2009, **38**, 671–683.
- 24 K. Nakamoto, *Infrared and Raman Spectra of Inorganic and Coordination Compounds*, Wiley, New York, 1986, p. 191.
- 25 J. Miyake, Y. Tsuji, A. Nagai and Y. Chujo, *Chem. Commun.*, 2009, 2183–2185.
- 26 S. Li, L. He, F. Xiong, Y. Li and G. Yang, *J. Phys. Chem. B*, 2004, **108**, 10887.
- 27 J. J. Vittal, Hydrogen-bonded coordination polymeric structures, in the book *Frontiers in Crystal Engineering*, ed. E. R. T. Tiekink and J. J. Vittal, Wiley, ch. 12, 2006, pp. 297–319.

